Subcortical connectivity correlates selectively with attention's effects on spatial choice bias

Varsha Sreenivasan[a,1] and Devarajan Sridharan[a,1]

[a]Centre for Neuroscience, Indian Institute of Science, 560012 Bangalore, India

Edited by Michael E. Goldberg, Columbia University, New York, NY, and approved August 1, 2019 (received for review February 16, 2019)

Neural mechanisms of attention are extensively studied in the neocortex; comparatively little is known about how subcortical regions contribute to attention. The superior colliculus (SC) is an evolutionarily conserved, subcortical (midbrain) structure that has been implicated in controlling visuospatial attention. Yet how the SC contributes mechanistically to attention remains unknown. We investigated the role of the SC in attention, combining model-based psychophysics, diffusion imaging, and tractography in human participants. Specifically, we asked whether the SC contributes to enhancing sensitivity (d′) to attended information, or whether it contributes to biasing choices (criteria) in favor of attended information. We tested human participants on a multialternative change detection task, with endogenous spatial cueing, and quantified sensitivity and bias with a recently developed multidimensional signal detection model (m-ADC model). At baseline, sensitivity and bias exhibited complementary patterns of asymmetries across the visual hemifields: While sensitivity was consistently higher for detecting changes in the left hemifield, bias was higher for reporting changes in the right hemifield. Remarkably, white matter connectivity of the SC with the neocortex mirrored this pattern of asymmetries. Specifically, the asymmetry in SC–cortex connectivity correlated with the asymmetry in choice bias, but not in sensitivity. In addition, SC–cortex connectivity strength could predict cueing-induced modulation of bias, but not of sensitivity, across individuals. In summary, the SC may be a key node in an evolutionarily conserved network for controlling choice bias during visuospatial attention.

attention components | sensitivity | choice bias | superior colliculus connectivity | asymmetry

Attention is an evolutionarily conserved cognitive capacity that enables the selection of behaviorally relevant information for prioritized sensory processing and decision-making (1, 2). While previous studies have extensively investigated the role of cortical brain regions in attention (3), comparatively little is known of subcortical contributions. Here, we investigate the role of the superior colliculus (SC), an evolutionarily conserved subcortical structure known to be important for directing eye movements (4) that has also been shown to play a role in controlling attention (5–13). Specifically, we investigate the role of the SC in controlling 1 of 2 key components of attention: perceptual sensitivity–enhanced sensory processing of the attended stimulus and choice bias, or selective gating of sensory information from the attended location for guiding behavioral decisions (14, 15).

Whether distinct cortical and subcortical regions mediate sensitivity and bias enhancement during attention is a topic of active research (14–16). Few studies have investigated this question in the neocortex. Two recent studies suggested that, while visual cortex (area V4) neurons selectively encode sensitivity modulation, the prefrontal cortex contains mixed neural populations that encode both sensitivity and bias modulations (14, 16). Similarly, other studies have suggested a role for the lateral intraparietal area in controlling bias in an overt attention task (3). In contrast, few studies have directly investigated the role of the subcortical SC in controlling sensitivity versus bias during attention tasks.

Manipulation of SC activity, either with focal microstimulation or with focal inactivation, produces systematic behavioral effects in attention tasks (17–20). For instance, 2 seminal studies (19, 21) showed that focal microstimulation of the SC produced attention-like shifts toward the receptive field location encoded by the stimulated SC neurons, whereas SC inactivation produced spatial attention deficits, as evidenced by an inability to detect changes in target features, particularly in the presence of foil (distractor) stimuli (18, 20). Using a model-based approach to reexamine these experimental data, a recent study (15) concluded that the behavioral effects of these SC manipulations were consistent with a selective role of the SC in controlling choice bias. This finding has been supported (22–24), as well as challenged (18, 25), by recent studies. The role of the SC in controlling sensitivity versus bias thus remains a topic of active debate.

Here, we addressed this question by investigating the neuroanatomical correlates of sensitivity and bias in the human SC with a combination of model-based psychophysics, diffusion MRI, and tractography of the SC. Sensitivity and bias were quantified using a multidimensional signal detection model (m-ADC model; refs. 15 and 26), with behavioral data from an endogenous attention task. These behavioral parameters were then correlated with participants' SC connectivity profiles. The results provide converging evidence for a selective role of the human SC in controlling choice bias during endogenous visuospatial attention.

Results

We employed 2 parallel approaches to test the link among SC connectivity, sensitivity, and bias. First, we quantified hemifield

Significance

Forebrain mechanisms of visuospatial attention have been widely studied. Yet, how the midbrain contributes to attention remains comparatively unknown. Here, we examined the role of the superior colliculus (SC), a vertebrate midbrain structure, in attention. Does the SC control sensitivity to attended information, or enable biasing choices toward attended information, or both? We mapped structural connections of the human SC with neocortical regions and found that the strengths of these connections correlated with, and were strongly predictive of, individuals' choice bias, but not sensitivity. Taken together with previous animal studies, our results suggest that the human SC may play an evolutionarily conserved role in controlling choice bias during visual attention.

Author contributions: D.S. designed research; V.S. performed research; V.S. analyzed data; and V.S. and D.S. wrote the paper.

The authors declare no conflict of interest.

This article is a PNAS Direct Submission.

Data deposition: The data reported in this paper, the code for analyses, and a high-quality version of Fig. 3 have been deposited in figshare (DOI: 10.6084/m9.figshare.8082245).

[1]To whom correspondence may be addressed. Email: varshas@iisc.ac.in or sridhar@iisc.ac.in.

This article contains supporting information online at www.pnas.org/lookup/suppl/doi:10.1073/pnas.1902704116/-/DCSupplemental.

First published September 6, 2019.

asymmetries in behavioral sensitivity and bias at baseline, and estimated the correlation with asymmetry in the SC's anatomical connectivity with the cortex and subcortex. Second, we quantified the modulation of sensitivity and bias by endogenous cueing and, again, measured their respective SC connectivity correlates.

Systematically Higher Bias for Right Visual Hemifield Choices. We quantified hemifield asymmetries in sensitivity and bias by acquiring behavioral data from 22 participants (group 1; *SI Appendix*, *SI Methods*); these participants performed a 2-alternative orientation change detection or 2-ADC task (Fig. 1*A* and *SI Appendix*, *SI Methods*). Briefly, participants detected and localized a change in orientation in 1 of 2 gratings that appeared in opposite visual hemifields. Participants indicated whether the change occurred in the left hemifield grating, in the right hemifield grating, or in neither grating (no change), using 3 distinct button-press responses (*SI Appendix*, *SI Methods* and Fig. S1*A*). Attention was directed to 1 of these 2 locations endogenously, with a spatial cue (75% cue validity; *SI Appendix*, *SI Methods*). Participants' responses were organized into 3 × 3 stimulus-response contingency tables (*SI Appendix*, Fig. S1 *B*, *Right* and *SI Appendix*, *SI Methods*), and psychophysical measures of sensitivity (d′), and criteria (c) were estimated by fitting the recently developed m-ADC model to conditional response probabilities in the contingency table (15, 26). The m-ADC model extends the conventional signal detection theory framework to multiple dimensions (Fig. 1*B*; described in detail in *SI Appendix*, *SI Methods*). Signal distributions, corresponding to change events at each location, were modeled as bivariate Gaussians with nonzero mean and unit variance along orthogonal axes, each representing sensory evidence at 1 of the 2 locations (Fig. 1 *B*, red and blue circles). The noise distribution, corresponding to the no change event, was modeled as a bivariate Gaussian with zero mean and unit variance (Fig. 1 *B*, black circle). Change detection sensitivity at each location (d'_C or d'_{UC}) was measured as the difference between the signal and noise distribution means along the corresponding axis. A decision surface, comprising 3 intersecting lines (Fig. 1 *B*, thick gray lines) divided the 2-dimensional decision space into 3 nonoverlapping decision zones. The decision surface was parametrized by 2 criteria (c_C and c_{UC}), one for each location. In the *SI Appendix* (*SI Appendix*, *SI Methods*), we describe how sensitivity (d′) and criteria at each location are related to and can be estimated from response proportions in the contingency table. We employed the choice criterion (b_{cc} = c-d′/2) as a measure of choice bias toward each location (27). Note that a lower choice criterion signifies a higher bias for reporting changes at that location. Responses were provided through distinct types of button-press configurations across subjects to avoid the confounding effects of oculomotor or manual response biases (*SI Appendix*, Fig. S1*A* and *SI Methods*).

First, we confirmed established results of endogenous cueing on behavioral metrics: On average, cueing increased hit rates and decreased reaction times, indicating that subjects reliably employed the spatial cue to direct their attention (*SI Appendix*, Fig. S1*C*; hit rate [HR]: cued = 71.1 ± 1.7%, uncued = 41.1 ± 3.6% [$P < 0.001$]; reaction time [RT]: cued = 651 ± 38 ms, uncued = 815 ± 37 ms, mean ± standard error of mean [SEM] [$P < 0.001$]). Similarly, cueing enhanced both sensitivity and bias at the cued location (Fig. 1*C*; d′: cued = 1.48 ± 0.10, uncued = 0.77 ± 0.13 [$P < 0.001$]; b_{cc}: cued = −0.24 ± 0.07, uncued = 0.46 ± 10, mean ± SEM [$P < 0.001$ Wilcoxon signed rank test]), in line with previous findings (28). Goodness-of-fit testing indicated that the m-ADC model fit individual participants' data well (randomization test; median P value = 0.795; range = 0.478 to 0.988; *SI Appendix*, Fig. S1*B*).

Nevertheless, we observed striking asymmetries in the average values of sensitivity and bias across the visual hemifields (average

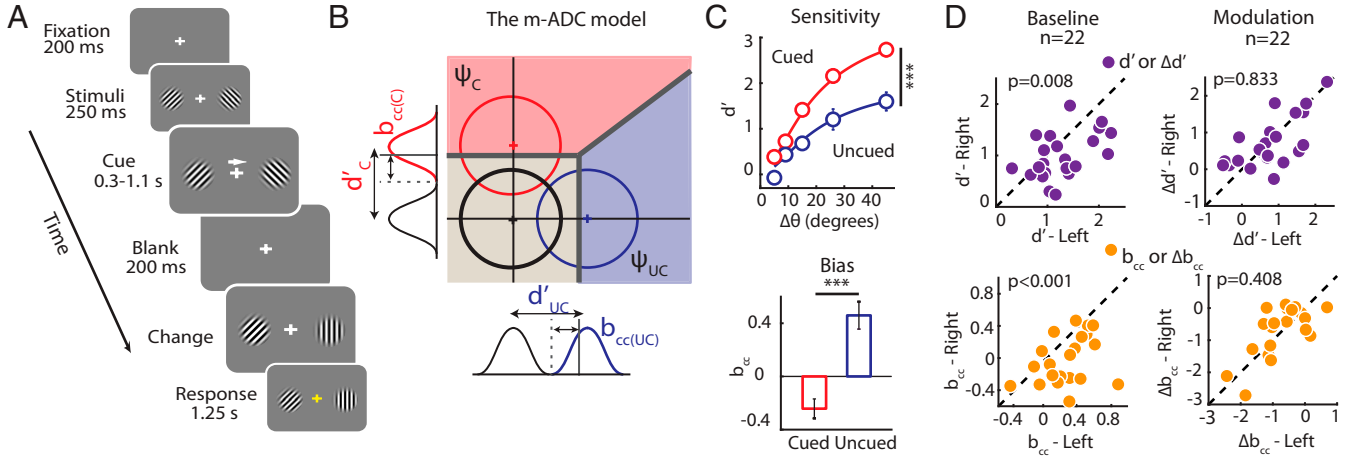

Fig. 1. Higher choice bias for right visual hemifield events. (*A*) Schematic of the endogenous attention task. After initial fixation, 2 grating stimuli appeared, one in each hemifield. After an interval of 250 ms, a spatial cue (central arrow) indicated the location at which change was more likely (cue validity: 75%). After a random interval (exponentially distributed), the gratings were blanked for 200 ms. On reappearance, either 1 of the 2 gratings had changed in orientation or neither had changed. Subjects indicated which of the 3 events (change in left grating orientation, right grating orientation, or no change) occurred on each trial. (*B*) Schematic of a two-dimensional signal detection (2-ADC) model for distinguishing sensitivity from bias effects of endogenous cueing of attention (15). Signal evidence at each location (cued/uncued) is represented along orthogonal axes. Colored circles: bivariate Gaussian decision variable distributions for changes at the cued (C, red) and uncued (UC, blue) locations. Black circle: decision variable distribution corresponding to "no change" trials. Thick gray lines: decision boundaries that divide the decision space into 3 decision zones: change at cued location (red shading), uncued location (blue shading), or no change (gray shading). One-dimensional signal and noise distributions for each location are indicated as marginals alongside each axis. (*C*, *Top*) Average psychophysical function across subjects ($n = 22$) showing perceptual sensitivity (d′) as a function of orientation change angle (Δθ) at the cued (red) and uncued (blue) locations. (*Bottom*) Mean choice criterion (b_{cc}) for reporting a change at the cued (red) or uncued (blue) locations. Note that choice criterion is a measure of bias and inversely related to it (see *Systematically Higher Bias for Right Visual Hemifield Choices*). Open circles: average d′. Curves: sigmoidal fits. Error bars: SEM. In some cases, error bars are smaller than the sizes of the respective symbols. ***$P < 0.001$. (*D*, *Left* and *Top*) Sensitivity (d′; purple dots) for detecting changes, at baseline, in the left (*x* axis) versus right (*y* axis) hemifields, as measured with the 2-ADC model ($n = 22$). (*Left* and *Bottom*) Same as in *Top*, but showing bias for reporting changes (b_{cc}; yellow dots). (*Right*) Same as in the *Left*, but for attentional modulation of sensitivity ($\Delta d' = d'_{cued} - d'_{uncued}$; purple) and bias ($\Delta b_{cc} = b_{cc\text{-}cued} - b_{cc\text{-}uncued}$; yellow). Filled circles: individual subjects. Dashed line: line of equality. *P* values denote significance for differences in behavioral metrics between left and right hemifields (asymmetry).

across cued and uncued trials; *SI Appendix, SI Methods*). Sensitivity for detecting changes was higher on the left compared with the right visual hemifield (Fig. 1*D*; d′: left = 1.28 ± 0.11; right = 0.99 ± 0.05; $P = 0.008$, Wilcoxon signed rank test). In contrast, choice bias was greater (b_{cc} was lower) for reporting changes on the right compared with the left hemifield (Fig. 1*D*; b_{cc}: left = 0.27 ± 0.07; right = −0.0006 ± 0.07; $P < 0.001$). Nevertheless, despite these robust hemifield asymmetries in average parameter values, the magnitudes of both sensitivity and bias modulation by endogenous cueing were not significantly different across hemifields (Fig. 1*D*; Δd′ [cued–uncued]: left = 0.76 ± 0.17, right = 0.73 ± 0.15; Δb_{cc} [cued–uncued]: left = −0.80 ± 0.15, right = −0.70 ± 0.16). In other words, both Δd′ and Δb_{cc} were significantly different from zero in both hemifields ($P < 0.001$, signed rank test), but both Δd′ and Δb_{cc} magnitudes were not significantly different across hemifields ($P > 0.05$).

We performed 3 control experiments and analyses to confirm the validity of these findings. First, we replicated these results in another group of $n = 34$ participants (group 3) performing a variant of the same task (*SI Appendix, SI Methods, SI Results*, and Fig. S1*D*). Second, to verify that response biases resulting from dominant hand use did not contribute to these results, we conducted a control experiment with $n = 10$ participants (group 4; *SI Appendix, SI Methods*) who performed the same attention task, but responded with their nondominant hand; we obtained the same results (*SI Appendix, SI Methods, SI Results*, and Fig. S8 *A* and *B*). Third, we fit a similarity choice model (29) to the participants' behavioral responses, and again observed robust hemifield asymmetries in sensitivity and choice bias (*SI Appendix, SI Results, Comparison of the m-ADC model with the similarity choice model* and *SI Appendix*, Fig. S5 *A–C*).

Taken together, these results reveal a robust dissociation between asymmetries in behavioral components of attention (sensitivity and bias) at baseline. The asymmetry in sensitivity is consistent with previous reports of a selective left-hemifield advantage during visuospatial attention (30–32).

Stronger SC Connectivity with Left Hemispheric Cortex. We asked whether the observed hemifield asymmetries in sensitivity and bias would have an underlying basis in neuroanatomical connectivity of the SC. As a first step, we quantified hemispheric asymmetries in the connectivity of the SC with various cortical and subcortical brain regions.

We analyzed diffusion MRI data from $n = 82$ participants, 22 of whom comprised the behavioral group described here (group 1). Sixty additional participants' data were drawn from the Human Connectome Project database (group 2; *SI Appendix, SI Methods*) (33). For each participant, we tracked streamlines between the SC (*SI Appendix*, Fig. S6*B*) and 34 cortical regions of interest (ROIs), with the Desikan-Killiany atlas (*SI Appendix*, Table S1 and Fig. S6*A*; ref. 34). The strength of connectivity for each streamline was quantified, using an established filtering algorithm (SIFT2; *SI Appendix, SI Methods*) (35). We also validated SC–cortex connection weights estimated using our approach (*SI Appendix*, Fig. S2 *A* and *B*) with previous reports (36–38) (*SI Appendix, SI Results, Validating SC-cortex connectivity asymmetries*).

SC connectivity with the cortex exhibited clear laterality, both voxelwise (Fig. 2*A*) and region-wise (Fig. 2*B*). Average connection weights with cortical regions in the left hemisphere were systematically higher than those with the corresponding regions in the right hemisphere in a majority of the ROIs (Fig. 2 *B*, *Top*; $P < 0.001$, $n = 22$; group 1). These asymmetries were also apparent when examining SC connection weights to individual cortical ROIs (e.g., superior temporal ROI; Fig. 2 *C*, *Top*; $P < 0.001$), but did not occur in all regions (*SI Appendix*, Fig. S2 *D* and *E*). We replicated these findings again in dMRI scans from a second group of subjects ($n = 60$; group 2-HCP database). Again, we observed significant hemispheric asymmetries in SC connection weights with a majority of the cortical regions (Fig. 2 *B*, *Bottom*; $P < 0.001$), as well as significant hemispherical asymmetries in specific cortical regions (Fig. 2 *C*, *Bottom*; superior temporal ROI; $P = 0.003$).

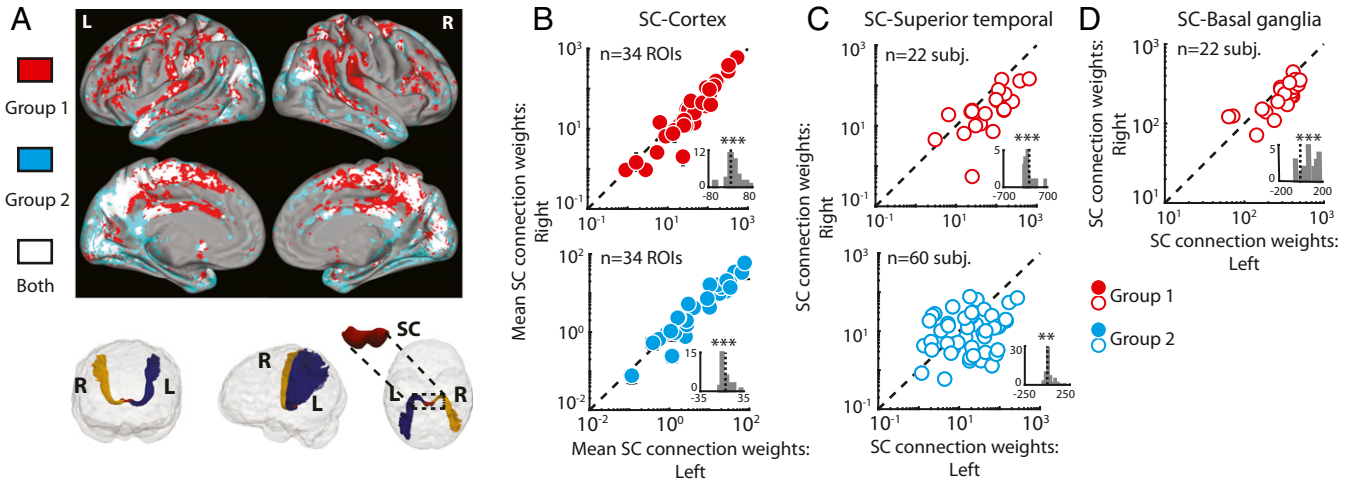

Fig. 2. Stronger superior colliculus (SC) connectivity with left hemispheric cortex. (*A*, *Top*) Thresholded surface maps (averaged across subjects) showing the voxelwise distribution across the cortex of connection weights with the SC. (*Left* and *Right*) Left and right hemispheres, respectively. (*Top* and *Bottom*): Lateral and medial views, respectively. Red: group 1 ($n = 22$), blue: group 2 ($n = 60$). Color scale is binary (*SI Appendix, SI Methods*). White voxels indicate regions of overlap between the 2 subject groups. (*Bottom*) 3D glass brain view showing white matter tracts between the SC and the inferior parietal cortex in the left (blue) and right (brown) hemispheres, for a representative subject. *Left*, *Middle*, and *Right* show coronal, sagittal and axial views, respectively. Black dashed line (*Inset*) 3D rendering of the SC ROI. (*B*) Subject-averaged connection weights of the SC with each of the 34 cortical regions (filled circles) in the left (*x* axis) versus right (*y* axis) hemispheres. (*Top*) Group 1 data; (*Bottom*) group 2 data. Error bars: SEM across subjects. Some error bars are smaller than the sizes of the respective symbols. Dashed line: line of equality. (*Inset*) Distribution of the difference in SC connection weights between left and right hemispheric regions ($w_{L\text{-}R}$). (*C*) Connection weights of the SC with an exemplar region (superior temporal ROI) in the left (*x* axis) versus right (*y* axis) hemispheres, for individual subjects (open circles). (*Top*) Group 1 data ($n = 22$); (*Bottom*) group 2 data ($n = 60$). Other conventions are as in *B*. (*D*) Same as in *C*, *Top*, but for connection weights of the SC with the basal ganglia ROI comprising the subthalamic nucleus, the substantia nigra, and the caudate nucleus. Other conventions are as in *C*. $^{**}P < 0.01$, $^{***}P < 0.001$.

To further ensure that these robust asymmetries were not a consequence of systematic biases in either our acquisition or analyses of the dMRI data, we tested for hemispheric asymmetries in a control region (V1, delineated with FreeSurfer; *SI Appendix*, *SI Methods*). Unlike the SC, the V1 exhibited mixed patterns of asymmetry in connectivity with other cortical regions (*SI Appendix*, Fig. S2 *E*, *Bottom*, and *SI Appendix*, S2 *F* and *G* and *SI Results, Validating SC-cortex connectivity asymmetries*). Moreover, we sought to replicate previous findings regarding asymmetries in fronto-parietal connections of 3 different subdivisions of the superior longitudinal fasciculus (SLF) (30). Our analyses reliably replicated previous reports of SLF connection asymmetries, thereby precluding systematic acquisition and analysis biases (*SI Appendix*, Fig. S7 *A* and *B* and *SI Results, Validating SC-cortex connectivity asymmetries*).

Finally, we asked whether connectivity asymmetries were confined to SC–cortex connections or were also apparent in the SC's connections to other subcortical structures. In particular, the SC is known to exhibit strong connections to several nuclei in the basal ganglia, comprising the subthalamic nucleus (STN), the substantia nigra (SN), and the caudate nucleus (39). We combine the STN and SN into one region, the STN + SN. We analyzed the strength of SC connections to these basal ganglia nuclei. As with cortical connectivity, we also observed a strong leftward asymmetry in SC-basal ganglia connection weights (Fig. 2*D*; $P < 0.001$).

In summary, neuroanatomical connections of the SC with cortical regions, as well as with the basal ganglia, were strikingly asymmetric, exhibiting stronger connectivity with left-hemispheric compared with right-hemispheric regions. The leftward asymmetry was characteristic of several, but not all, SC–cortex connections, and was not observed in V1–cortex or the fronto-parietal (SLF) connections. Would these robust hemispheric asymmetries in SC connectivity correlate with hemifield asymmetries in behavioral metrics (sensitivity and bias)? We addressed this question next.

Asymmetry in SC Connectivity Correlates with Choice Bias Asymmetry. Before testing for the relationship of sensitivity and bias asymmetries with asymmetry in SC connectivity across participants, we first asked whether these metrics would themselves be stable and reliably quantified in individual participants over the course of several days. A test-retest reliability analysis revealed significant correlations in sensitivity and bias values across several days (*SI Appendix*, Fig. S1*E*, *SI Methods*, and *SI Results, Evaluating the stability of sensitivity and bias over time*). Next, we combined the 34 ROIs in each hemisphere into 11 major aggregate ROIs (aROIs) on the basis of their anatomical proximity (*SI Appendix*, Table S1 and Fig. S2*C*); we also combined the basal-ganglia regions into a 12th aROI (*SI Appendix*, Table S1 and Fig. S2*C*). The aggregate ROI definition was agnostic to subsequent results and limited the need for stringent multiple comparisons correction (*SI Appendix*, *SI Methods*).

We next asked whether these hemifield asymmetries in sensitivity and bias were correlated with hemispheric asymmetries in SC–cortex structural connectivity. To test this, we analyzed data from group 1 ($n = 22$) participants for whom both attention task data and dMRI data were available. We first quantified hemifield asymmetries in sensitivity and bias as the difference in the value of these parameters across the left and right hemifields ($\delta_{L\text{-}R}$; *SI Appendix*, *SI Methods*). Similarly, we quantified hemispheric asymmetry in structural connectivity as a ratio of difference in the value of regional connectivity weights across the left and right hemispheres to their sum ($MI_{R\text{-}L}$; *SI Appendix*, *SI Methods*). We then proceeded to test the link between these behavioral and brain metrics in 2 stages.

First, we examined correlations between the asymmetries in behavioral metrics and connectivity ($\delta_{L\text{-}R}$ and $MI_{R\text{-}L}$). After multiple comparisons correction, we identified a strong positive correlation between asymmetry in the SC–Cingulate aROI connection weights and asymmetry in choice bias (Fig. 3 *A*, *Bottom*; δb_{cc}; $r = 0.625$; $P = 0.002$; Benjamini-Hochberg correction; *SI Appendix*, *SI Methods*). In contrast, connectivity asymmetries in none of the aROIs showed significant correlations with sensitivity asymmetries (Fig. 3 *A*, *Middle*; $\delta d'$; $r = -0.355$, $P = 0.105$).

Second, we tested whether the asymmetries in SC connectivity in individual participants could predict their (respective) hemifield asymmetries in sensitivity or bias. We performed a leave-one-out regression analysis based on support-vector-machines, using SC connectivity asymmetries ($MI_{R\text{-}L}$) to 34 cortical regions, the STN + SN, and caudate nucleus (36 ROIs total) as features and predicted individual subjects' sensitivity and bias asymmetries ($\delta_{L\text{-}R}$; Fig. 3*B* and *SI Appendix*, *SI Methods*). SC connection asymmetries robustly predicted individual behavioral asymmetries in bias (Fig. 3 *C*, *Left Bottom*; $r = 0.743$; $P < 0.001$), but not in sensitivity (Fig. 3 *C*, *Left Top*; $r = -0.104$; $P = 0.645$). We quantified the contribution of each region to the linear prediction, using the magnitude of their regression weights (β), and found that SC connections with frontal and cingulate cortex (Fig. 3 *C*, *Right*), contributed strongly to the predictions (*SI Appendix*, *SI Methods*).

Finally, a control analysis revealed that V1 asymmetries neither correlated with nor were predictive of sensitivity and bias asymmetries (*SI Appendix*, *SI Results* and Fig. S3*A*). Other control analyses, based on reaction times (*SI Appendix*, *SI Results* and Fig. S9*B*), based on SLF connectivity (*SI Appendix*, *SI Results* and Fig. S7*C*), and based on the similarity choice model (*SI Appendix*, *SI Results* and Fig. S5*D*), are described in the *SI Appendix*.

In sum, interhemispheric asymmetries in the strength of SC connectivity with the cingulate aROI correlated strongly with hemifield asymmetries in choice bias, but not sensitivity across individuals. In addition, SC–cortex connectivity asymmetries could robustly predict interindividual differences in hemifield asymmetries in bias, but not sensitivity. Taken together, these results indicate a strong and selective relationship between human SC connectivity asymmetries and asymmetries in one of the behavioral components of attention (bias).

Average SC Connectivity Correlates with Choice Bias Modulation by Cueing. Whereas SC connectivity asymmetry and bias asymmetry were correlated at baseline, we tested whether SC connectivity also correlated with the modulation of bias by endogenous cueing across individual subjects. As before, we tested this hypothesis with a 2-stage approach.

First, we computed the modulation of sensitivity and bias ($\Delta d'$, Δb_{cc}; *SI Appendix*, *SI Methods*) by endogenous cueing and correlated these quantities with average SC connection weights to each aROI (weights averaged across hemispheres). Several SC–cortex and SC–basal ganglia connections showed strong, significant correlations with bias modulation (e.g., SC–parietal, Δb_{cc}: $r = -0.519$; $P = 0.013$; Fig. 3 *D*, *Bottom*); note that these correlations are negative because a more negative Δb_{cc} value indicates a stronger modulation of bias by endogenous cueing. In contrast, SC–cortex connectivity weights did not show significant correlations with sensitivity modulation (Fig. 3 *D*, *Top*). Interestingly, the strength of SC–cortex connectivity did not correlate with average values of bias (or sensitivity) across subjects (b_{cc}: $r = -0.159$ [$P = 0.479$]; d': $r = -0.058$ [$P = 0.797$]), indicating that these correlations were not due to interindividual differences in the overall values of sensitivity and bias parameters.

Second, we tested whether SC connectivity could predict interindividual differences in the modulation of sensitivity or bias by endogenous cueing. Here, we employed average SC–cortex and SC–basal ganglia connection strengths (36 ROIs) as features in a support-vector regression to predict $\Delta d'$ and Δb_{cc}. We found that SC connectivity robustly predicted variations in bias modulation (Δb_{cc}: $r = 0.605$; $P = 0.003$; Fig. 3 *E*, *Left Bottom*). Connectivity with various regions in the frontal, parietal, cingulate, and temporal cortices contributed to these behavioral predictions (Fig. 3 *E*, *Right*). In contrast, the same analysis failed to accurately predict interindividual variation in sensitivity modulation by cueing ($\Delta d'$: $r = 0.162$; $P = 0.470$; Fig. 3 *E*, *Left Top*).

Interestingly, a control analysis revealed that V1 connectivity correlated with modulation of sensitivity ($\Delta d'$: $r = 0.477$; $P = 0.025$), but not with modulation of bias (Δb_{cc}; $r = 0.306$; $P = 0.167$;

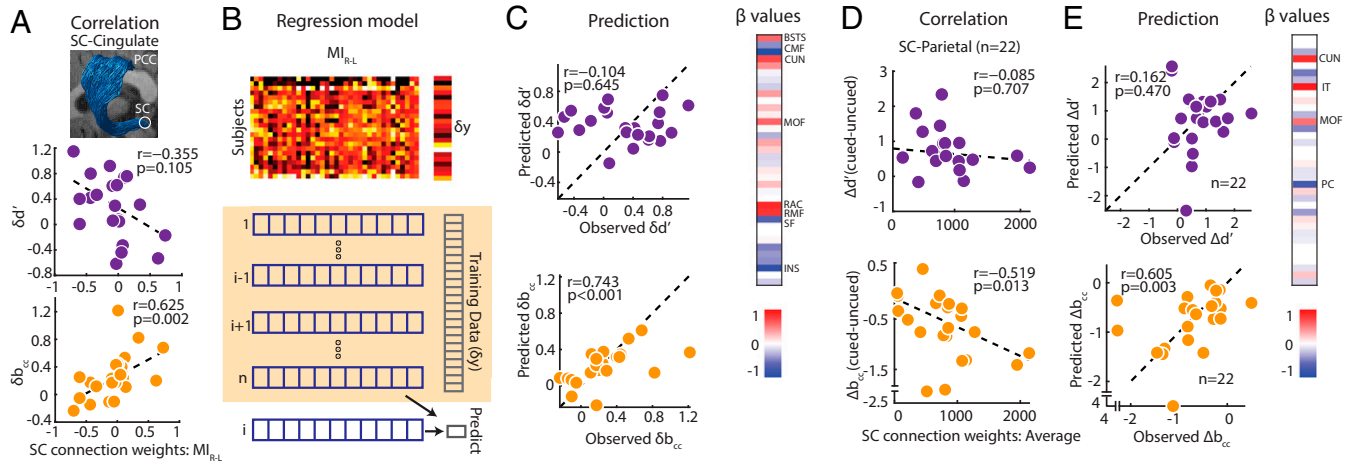

Fig. 3. Asymmetry in SC connectivity correlates selectively with choice bias asymmetry and average SC connectivity correlates selectively with choice bias modulation. (*A*, *Top*) Representative white matter tracts between the SC and the posterior cingulate cortex (PCC). (*Bottom*) Hemispheric asymmetry in the SC-Cingulate aROI connection weights (MI_{R-L}; *SI Appendix*, *SI Methods*; *x* axis), plotted against hemifield asymmetry in sensitivity (δd′; *Top*, purple data) and bias ($δb_{cc}$; *Bottom*, yellow data). Filled circles: individual subjects. Dashed line: line of best fit. (*B*) Schematic of the algorithm for predicting each subject's hemifield asymmetry in sensitivity (δd′) or bias ($δb_{cc}$), using SC connectivity asymmetry. The n × m (m = 36 ROIs; *n* = 22 subjects) feature matrix (MI_{R-L}; *Top*) was used to predict each subject's hemifield asymmetry in sensitivity (δd′) or bias ($δb_{cc}$), using support vector regression, with a leave-one-subject out approach (*Bottom*). (*C*) (*Left*) Observed (*x* axis) versus predicted (*y* axis) asymmetries for sensitivity (δd′; *Top*, purple data) and bias ($δb_{cc}$; *Bottom*, yellow data) across individual subjects. Dashed line: line of equality. *r* and *P* values indicate correlation between observed and predicted values. (*Right*) Normalized regression coefficients (β) for predicting bias asymmetries. Labels indicate connections with |β|>0.5 (*SI Appendix*, Fig. S2*C* and *SI Methods*). (*D*, *Top*) Average SC–parietal cortex aROI connection weights (*x* axis) plotted against the average modulation of sensitivity (Δd′; purple data; *y* axis) with endogenous cueing. Filled circles: individual subjects. Dashed line: line of best fit. (*Bottom*) Same as in the *Top* but for modulation of bias ($Δb_{cc}$; yellow data). Other conventions are as in the *Top*. (*E*, *Left*) Same as in *C*, *Left*, but showing observed (*x* axis) versus predicted (*y* axis) modulations of sensitivity (Δd′; *Top*, purple data) and bias ($Δb_{cc}$; *Bottom*, yellow data) by endogenous cueing. (*Right*) Same as in *C*, *Right*, but showing the normalized coefficients (β) assigned to individual connections (features) for predicting modulations of bias. Other conventions are as in *C*.

SI Appendix, Fig. S3*B* and *SI Results, V1 connectivity: correlation with behavior*).

Taken together, the results reveal that SC connectivity was strongly correlated with and predictive of interindividual variations in the modulation of choice bias, but not sensitivity, (*SI Appendix*, Fig. S4*A*) by endogenous cueing of attention. The results confirm a strong and specific link between SC connectivity and the choice bias component of endogenous attention.

Discussion

The neural mechanisms of attention are being actively investigated in a variety of species (1, 40). Yet most studies have largely focused on the cortex, and particularly the fronto-parietal network (41), and little is known about how evolutionarily conserved subcortical regions contribute to attention (15, 42). Recent studies suggest that the SC is a key node in a midbrain attention network (18–20, 42). However, the precise role of the SC in attention, in terms of controlling sensitivity versus bias, remains debated (22, 25). In this study, we performed a detailed neuroanatomical characterization of the human SC's connectivity, with diffusion imaging and tractography, to show that the human SC exhibits patterns of anatomical connectivity with cortical and subcortical structures that are consistent with its role in selectively modulating choice bias during attention.

Attention, typically, is not uniformly engaged across the visual field: A left hemifield advantage has been routinely measured in paradigms such as line bisection tasks (30). Our study indicates that this left hemifield advantage occurs for only the perceptual sensitivity component of attention. In contrast, choice bias for reporting changes exhibited a right hemifield advantage, suggesting dissociable neural mechanisms for each component. Paralleling these behavioral asymmetries, hemispheric differences in structural connectivity and their correlation with attention behaviors have also been documented (30). Our results indicate that hemispheric asymmetries in connectivity of the SC may underlie hemifield asymmetries in choice bias. Specifically, we observed strong correlation between asymmetry in cingulate–SC connectivity and hemifield asymmetry in choice bias (Fig. 3): stronger SC connectivity with the cingulate cortex in the right hemisphere correlated with a higher bias toward the right (ipsilateral) hemifield. This pattern is consistent with the hypothesis that the cingulate–SC connection is functionally inhibitory, such that greater right cingulate–SC connectivity would reduce bias toward the left (contralateral) visual field, thereby producing a higher bias toward the right (ipsilateral) visual field.

The connectivity of the SC has been extensively characterized using both tracer studies in nonhuman primates (36, 37) and diffusion imaging in humans (38, 39). Retrograde tracing in macaques has identified strong descending projections from the posterior parietal cortex to the SC (36, 43). These findings have been confirmed in human diffusion imaging studies, which have indicated that a specific subregion of the parietal cortex projects to the SC (38). In addition, stimulation studies indicate that parietal cortex neurons can be activated by antidromic stimulation at the SC (43). In our data, SC connections to the parietal cortex were among the strongest across 2 different groups of human participants (Fig. 2 and *SI Appendix*, Fig. S2); these connections likely reflect direct descending projections from the parietal cortex to the SC (44). Strong asymmetric descending projections to the SC are likely to asymmetrically activate SC neurons, leading to hemifield asymmetries in behavior. Specifically, our findings lead to the testable hypothesis that inactivating the left SC would lead to stronger bias deficits in the right hemifield, rather than vice versa. Moreover, recent neuroimaging studies have indicated strong functional connectivity of the primate SC, both with the frontal lobe (45) as well as with the temporal lobe during a spatial attention task (42). Our findings suggest a neuroanatomical basis for these observations (Fig. 2).

The interindividual variability in SC connectivity with several cortical regions correlated with and was predictive of the interindividual differences in the modulation of choice bias by endogenous cueing of attention. The magnitude of this choice bias modulation reflects the subjects' ability to flexibly adjust choice criteria across the cued and uncued locations based on

cue validity (28). SC–cortex connectivity may therefore index subjects' abilities to flexibly adjust decision strategies (criteria) based on task-relevant information. Interestingly, SC connectivity did not correlate with and could not predict interindividual differences in sensitivity modulation. Furthermore, we were not able to predict interindividual differences in choice bias based on other cortico-cortical connections such as V1-frontal, V1-parietal, or (SLF) fronto-parietal connections.

These findings are consistent with a recent hypothesis regarding a selective role of the subcortex in mediating choice bias (ref. 15, but see ref. 25). In support of this hypothesis, recent studies have shown that reversible chemical inactivation of the SC in nonhuman primates and optogenetic activation of the basal ganglia neurons in mice produced strong effects on decisional biases while only minimally affecting sensitivity (18, 46). Moreover, our findings showed that the strength of the SC connection with the basal ganglia (caudate and STN + SN aROI) correlated selectively with modulations of bias (*SI Appendix*, Fig. S4*A*). Nevertheless, it is also possible that sensitivity and bias changes are mediated by overlapping brain structures that are modulated to different extents in different species (16).

More generally, our findings on structure–behavior relationships motivate other key questions on white matter plasticity and its consequences for attention. Can subjects learn to selectively modulate one component of attention and not the other? Would such learning generate structural changes in specific connections? Can structural plasticity induced by neurostimulation, in turn, alter only 1 of the 2 components of attention? Addressing these questions could provide deeper insights into key mechanisms of selective attention in the brain.

Materials and Methods

All experiments were conducted in accordance with protocols approved by the Institute Human Ethics Committee, Indian Institute of Science, Bangalore. Informed written consent was obtained from each participant before the study. Detailed Methods are presented in the *SI Appendix*. All data discussed in the paper, including cortical and subcortical ROIs for each individual subject, as well as tracts showing connections of the SC with the cortex, and connection weights between every pair of regions, and relevant code, have been deposited into an online repository (47) for ready inspection and replication of the results.

ACKNOWLEDGMENTS. We thank John Duncan, Kendrick Kay, Sricharan Sunder, and Priyanka Gupta for their feedback on an earlier version of this manuscript, and Ankita Sengupta, Sanjna Banerjee, and Guruprasath Gurusamy for help with data collection. We would also like to thank HealthCare Global hospital for access to the MRI scanning facility. This research was funded by a Wellcome Trust/Department of Biotechnology India Alliance Intermediate fellowship [IA/I/15/2/502089], a Science and Engineering Research Board Early Career award [ECR/2016/000403], a Pratiksha Trust Young Investigator award, a Department of Biotechnology-Indian Institute of Science Partnership Program grant, a Sonata Software grant, and a Tata Trusts grant (to D.S.).

1. M. P. Eckstein *et al.*, Rethinking human visual attention: Spatial cueing effects and optimality of decisions by honeybees, monkeys and humans. *Vision Res.* **85**, 5–19 (2013).
2. R. J. Krauzlis, A. R. Bogadhi, J. P. Herman, A. Bollimunta, Selective attention without a neocortex. *Cortex* **102**, 161–175 (2018).
3. F. Arcizet, K. Mirpour, D. J. Foster, C. J. Charpentier, J. W. Bisley, LIP activity in the interstimulus interval of a change detection task biases the behavioral response. *J. Neurophysiol.* **114**, 2637–2648 (2015).
4. A. K. Moschovakis, The superior colliculus and eye movement control. *Curr. Opin. Neurobiol.* **6**, 811–816 (1996).
5. R. H. Wurtz, M. E. Goldberg, The primate superior colliculus and the shift of visual attention. *Invest. Ophthalmol.* **11**, 441–450 (1972).
6. M. E. Goldberg, R. H. Wurtz, Activity of superior colliculus in behaving monkey. II. Effect of attention on neuronal responses. *J. Neurophysiol.* **35**, 560–574 (1972).
7. A. A. Kustov, D. L. Robinson, Shared neural control of attentional shifts and eye movements. *Nature* **384**, 74–77 (1996).
8. R. M. McPeek, E. L. Keller, Deficits in saccade target selection after inactivation of superior colliculus. *Nat. Neurosci.* **7**, 757–763 (2004).
9. G. D. Horwitz, W. T. Newsome, Separate signals for target selection and movement specification in the superior colliculus. *Science* **284**, 1158–1161 (1999).
10. R. J. Krauzlis, D. Liston, C. D. Carello, Target selection and the superior colliculus: Goals, choices and hypotheses. *Vision Res.* **44**, 1445–1451 (2004).
11. J. Shires, S. Joshi, M. A. Basso, Shedding new light on the role of the basal ganglia-superior colliculus pathway in eye movements. *Curr. Opin. Neurobiol.* **20**, 717–725 (2010).
12. M. A. Basso, R. H. Wurtz, Modulation of neuronal activity in superior colliculus by changes in target probability. *J. Neurosci.* **18**, 7519–7534 (1998).
13. M. A. Basso, R. H. Wurtz, Modulation of neuronal activity by target uncertainty. *Nature* **389**, 66–69 (1997).
14. T. Z. Luo, J. H. R. Maunsell, Neuronal modulations in visual cortex are associated with only one of multiple components of attention. *Neuron* **86**, 1182–1188 (2015).
15. D. Sridharan, N. A. Steinmetz, T. Moore, E. I. Knudsen, Does the superior colliculus control perceptual sensitivity or choice bias during attention? Evidence from a multialternative decision framework. *J. Neurosci.* **37**, 480–511 (2017).
16. T. Z. Luo, J. H. R. Maunsell, Attentional changes in either criterion or sensitivity are associated with robust modulations in lateral prefrontal cortex. *Neuron* **97**, 1382–1393.e7 (2018).
17. J. Cavanaugh, R. H. Wurtz, Subcortical modulation of attention counters change blindness. *J. Neurosci.* **24**, 11236–11243 (2004).
18. A. Zénon, R. J. Krauzlis, Attention deficits without cortical neuronal deficits. *Nature* **489**, 434–437 (2012).
19. J. R. Müller, M. G. Philiastides, W. T. Newsome, Microstimulation of the superior colliculus focuses attention without moving the eyes. *Proc. Natl. Acad. Sci. U.S.A.* **102**, 524–529 (2005).
20. L. P. Lovejoy, R. J. Krauzlis, Inactivation of primate superior colliculus impairs covert selection of signals for perceptual judgments. *Nat. Neurosci.* **13**, 261–266 (2010).
21. R. H. Wurtz, J. E. Albano, Visual-motor function of the primate superior colliculus. *Annu. Rev. Neurosci.* **3**, 189–226 (1980).
22. T. B. Crapse, H. Lau, M. A. Basso, A role for the superior colliculus in decision criteria. *Neuron* **97**, 181–194.e6 (2018).
23. P. Grimaldi, S. H. Cho, H. Lau, M. A. Basso, Superior colliculus signals decisions rather than confidence: Analysis of single neurons. *J. Neurophysiol.* **120**, 2614–2629 (2018).
24. B. Odegaard *et al.*, Superior colliculus neuronal ensemble activity signals optimal rather than subjective confidence. *Proc. Natl. Acad. Sci. U.S.A.* **115**, E1588–E1597 (2018).
25. L. P. Lovejoy, R. J. Krauzlis, Changes in perceptual sensitivity related to spatial cues depends on subcortical activity. *Proc. Natl. Acad. Sci. U.S.A.* **114**, 6122–6126 (2017).
26. D. Sridharan, N. A. Steinmetz, T. Moore, E. I. Knudsen, Distinguishing bias from sensitivity effects in multialternative detection tasks. *J. Vis.* **14**, 16(2014).
27. J. D. Ingleby, Signal detection theory and psychophysics *J. Sound Vib.* **5**, 519–521 (1967).
28. S. Banerjee, S. Grover, S. Ganesh, D. Sridharan, Sensory and decisional components of endogenous attention are dissociable. *J. Neurophysiol.* 10.1152/jn.00257.2019 (2019).
29. V. Cane, R. D. Luce, *Individual Choice Behavior: A Theoretical Analysis* (Courier Corporation, 2006).
30. M. Thiebaut de Schotten *et al.*, A lateralized brain network for visuospatial attention. *Nat. Neurosci.* **14**, 1245–1246 (2011).
31. J. Charles, A. Sahraie, P. McGeorge, Hemispatial asymmetries in judgment of stimulus size. *Percept. Psychophys.* **69**, 687–698 (2007).
32. J. L. Bradshaw, G. Nathan, N. C. Nettleton, L. Wilson, J. Pierson, Why is there a left side underestimation in rod bisection? *Neuropsychologia* **25**, 735–738 (1987).
33. D. C. Van Essen *et al.*; WU-Minn HCP Consortium, The human connectome project: A data acquisition perspective. *Neuroimage* **62**, 2222–2231 (2012).
34. B. Fischl, FreeSurfer. *Neuroimage* **62**, 774–781 (2012).
35. R. E. Smith, J. D. Tournier, F. Calamante, A. Connelly, SIFT2: Enabling dense quantitative assessment of brain white matter connectivity using streamlines tractography. *Neuroimage* **119**, 338–351 (2015).
36. W. Fries, Cortical projections to the superior colliculus in the macaque monkey: A retrograde study using horseradish peroxidase. *J. Comp. Neurol.* **230**, 55–76 (1984).
37. W. Fries, Inputs from motor and premotor cortex to the superior colliculus of the macaque monkey. *Behav. Brain Res.* **18**, 95–105 (1985).
38. M. F. S. Rushworth, T. E. J. Behrens, H. Johansen-Berg, Connection patterns distinguish 3 regions of human parietal cortex. *Cereb. Cortex* **16**, 1418–1430 (2006).
39. P. Redgrave *et al.*, Interactions between the midbrain superior colliculus and the basal ganglia. *Front. Neuroanat.* **4**, 132 (2010).
40. D. Sridharan, J. S. Schwarz, E. I. Knudsen, Selective attention in birds. *Curr. Biol.* **24**, R510–R513 (2014).
41. M. Scolari, K. N. Seidl-Rathkopf, S. Kastner, Functions of the human frontoparietal attention network: Evidence from neuroimaging. *Curr. Opin. Behav. Sci.* **1**, 32–39 (2015).
42. A. R. Bogadhi, A. Bollimunta, D. A. Leopold, R. J. Krauzlis, Brain regions modulated during covert visual attention in the macaque. *Sci. Rep.* **8**, 15237 (2018).
43. M. Paré, R. H. Wurtz, Monkey posterior parietal cortex neurons antidromically activated from superior colliculus. *J. Neurophysiol.* **78**, 3493–3497 (1997).
44. E. Borra, M. Gerbella, S. Rozzi, S. Tonelli, G. Luppino, Projections to the superior colliculus from inferior parietal, ventral premotor, and ventrolateral prefrontal areas involved in controlling goal-directed hand actions in the macaque. *Cereb. Cortex* **24**, 1054–1065 (2014).
45. C. B. Field, K. Johnston, J. S. Gati, R. S. Menon, S. Everling, Connectivity of the primate superior colliculus mapped by concurrent microstimulation and event-related FMRI. *PLoS One* **3**, e3928 (2008).
46. L. Wang, K. V. Rangarajan, C. R. Gerfen, R. J. Krauzlis, Activation of striatal neurons causes a perceptual decision bias during visual change detection in mice. *Neuron* **97**, 1369–1381 (2018).
47. V. Sreenivasan, D. Sridharan, Subcortical connectivity correlates selectively with attention's effects on spatial choice bias. Figshare. https://dx.doi.org/10.6084/m9.figshare.8082245. Deposited 15 August 2019.